Integrated Microfluidic Systems for Molecular Diagnostics

A universal electrode platform for rapid diagnosis of urinary tract infections.

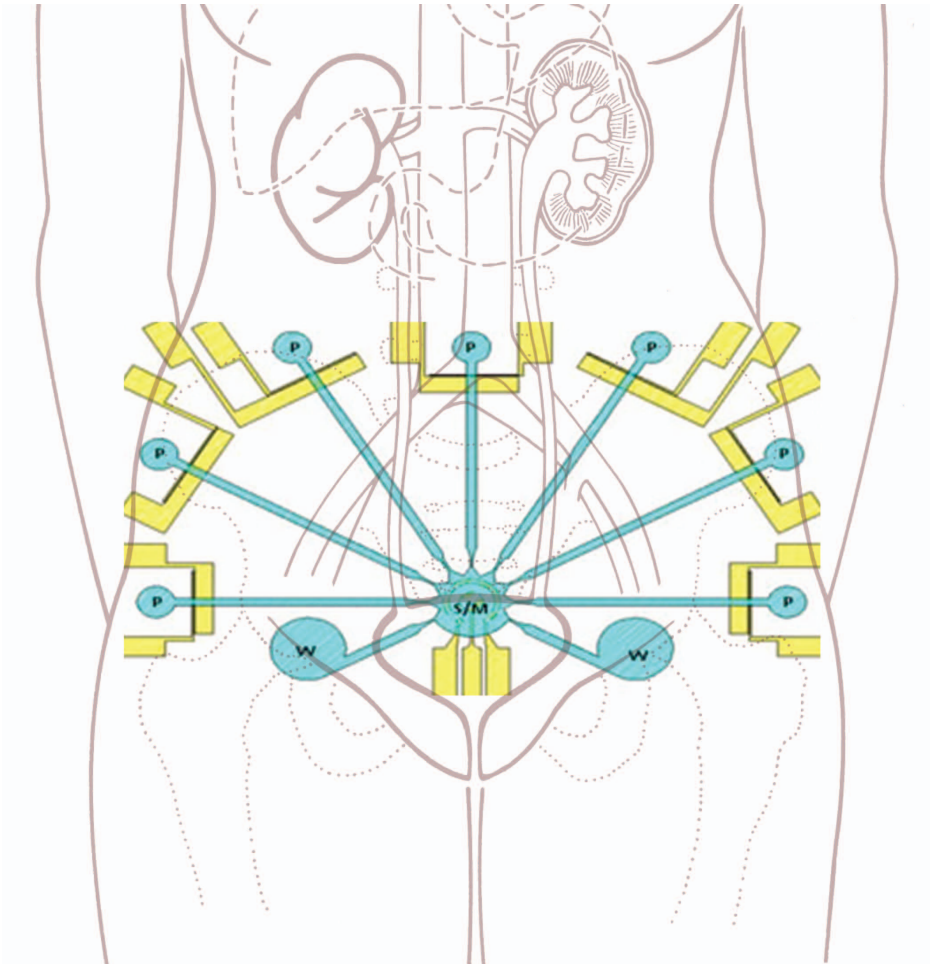

URINARY TRACT IMAGE IS COURTESY OF THE NATIONAL INSTITUTES OF HEALTH.

TRANSFORMING MICROFLUIDICS-based biosensing systems from laboratory research into clinical reality remains an elusive goal despite decades of intensive research. A fundamental obstacle in the development of fully automated microfluidic diagnostic systems is the lack of an effective strategy for combining multiple pumping, sample preparation, and detection modules into an integrated platform. In this article, we report a universal electrode approach, which incorporates dc electrolytic pumping, ac electrokinetic sample preparation, and electrochemical sensing based on a self-assembled monolayer (SAM) on a single microfluidic platform, to automate complicated molecular analysis procedures in nontraditional healthcare settings.

Using the universal electrode approach, major microfluidic operations required in molecular diagnostics, such as pumping, mixing, washing, and sensing, can be performed in a single platform. We demonstrate the universal electrode platform for detecting bacterial 16S rRNA, a

MANDY L. Y. SIN, VINCENT GAU, JOSEPH C. LIAO, AND P. K. WONG

Digital Object Identifier 10.1109/MNANO.2012.2237331
Date of publication: 5 February 2013

1932-4510/13/$31.00©2013IEEE

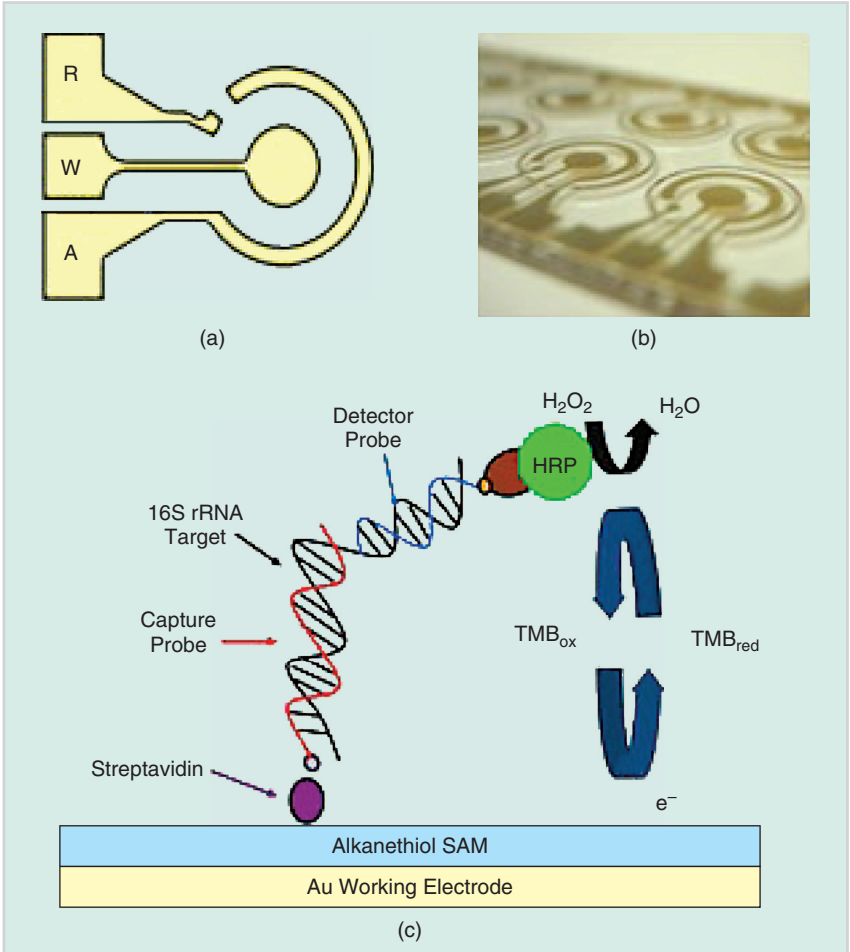

FIGURE 1 Electrochemical biosensor for bacterial 16S rRNA. (a) The concentric electrode configuration for electrochemical sensing. (b) The concentric electrode. (c) A schematic of the sandwich binding scheme for detecting bacterial 16S rRNA for urinary tract infection diagnosis.

phylogenetic marker, for more rapid diagnosis of urinary tract infections (UTIs). Since only electronic interfaces are required to operate the platform, the universal electrode approach represents an effective system integration strategy to realize the potential of microfluidics in molecular diagnostics at the point of care.

The realization of fully integrated microfluidic systems for molecular diagnostics remains an elusive goal despite intensive efforts in the past decades. Existing lab-on-a-chip devices often require bulky supporting equipment and have limited applicability in nontraditional healthcare settings (e.g., physician's offices and emergency departments). The implementation of fully automated lab-on-a-chip systems is fundamentally hindered by the difficulty of integrating multiple fluid manipulation and molecular sensing modularities, such as external pumps, pressure sources, mixers, and biosensors, in a robust and cost-effective manner [1]–[4]. Effective system integration strategies are required to fully utilize the potential of microfluidics in molecular diagnostics.

Several microfluidic system integration approaches, such as digital, multiphase, magnetic, optofluidic, centrifugal, and electrokinetic techniques, have been developed to meet the goal of implementing fully integrated lab-on-a-chip systems [1]. Among these techniques, electrokinetics is one of the most promising microfluidic platforms for point-of-care diagnostics because of its low power consumption, cost-effectiveness, simplicity in microelectrode fabrication, and advancement in a portable electronic interface [5], [6]. Recent efforts in electrokinetics have enabled various fundamental microfluidic operations, such as mixing, concentration, and separation, to be performed in high-conductivity physiological fluids [7]–[11]. Furthermore, electrokinetics can be implemented conveniently in electrochemical sensing platforms [9].

We have demonstrated an electrochemical biosensor based on SAM for detecting bacterial 16S rRNA and protein biomarkers [12]–[14]. The electrochemical biosensor is sensitive, specific, and rapid and represents a highly promising technology for point-of-care diagnostics of infectious diseases, such as UTIs [15]. We have demonstrated in situ electrokinetic enhancement directly on the electrochemical sensor [9]. Nevertheless, the manual assay has to be performed by trained personnel and is difficult to implement in resource-limited settings.

In this study, we develop a universal electrode approach toward the implementation of fully integrated microfluidic biosensing systems. In particular, we

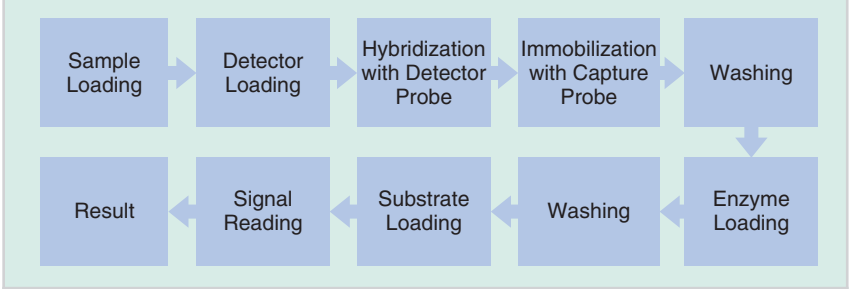

FIGURE 2 Procedure of the electrochemical assay for detecting bacterial 16S rRNA.

incorporate electrolytic pumping, electrokinetic sample preparation, and amperometric sensing using a set of universal electrode arrays to implement the entire molecular assay automatically. We show that the electrolytic pump allows effective fluid delivery and washing, and that ac electrokinetics enables mixing and assay enhancement directly on the electrochemical sensor electrode. Using pathogenic clinical isolates from patients with UTI, we demonstrate the applicability of the universal electrode approach by implementing the electrochemical assay for detecting bacterial 16S rRNA.

> The universal electrode approach represents an effective system integration strategy to realize the potential of microfluidics in molecular diagnostics at the point of care.

DESIGN AND FABRICATION

ELECTROCHEMICAL BIOSENSOR

The SAM-based electrochemical biosensor consists of a concentric electrode design with working (W), auxiliary (A), and reference (R) electrodes (Figure 1). The protocol of the electrochemical assay for bacterial 16S rRNA involves 1) sample loading, 2) detector probe loading, 3) hybridization, 4) immobilization, 5) washing, 6) enzyme loading, 7) washing, 8) substrate loading, and 9) signal reading (Figure 2) [16]. To implement the electrochemical assay, the target 16S rRNA is allowed to hybridize to a capture probe. The capture probe consists of a biotin tag and immobilizes the target 16S rRNA onto the streptavidin-coated working electrode surface. Unbound molecules can then be washed away. A detector probe is also added to the sensor. The detector probe is labeled with a fluorescein molecule for horseradish peroxidase binding [Figure 1(c)]. By loading the substrate H_2O_2 with tetramethylbenzidine as the electron transfer mediator, we can determine the concentration of the target 16S rRNA amperometrically.

ELECTROLYTIC PUMPING

The electrolytic micropump consists of a pair of asymmetric electrodes with widths of 100 and 2,000 μm (Figure 3). The electrode is separated by a gap of 100 μm. The electrodes were fabricated by evaporation of 50 nm of titanium (Ti), 150 nm of gold (Au), and 50 nm of titanium on glass substrate and were patterned by liftoff. The Ti–Au–Ti sandwich structure is chosen to endure high voltage for an extended period of time without damaging the electrodes in high-conductivity media [7]. A function generator (HP, 33120A) was used to generate the dc voltage signal. The 100-μm wide electrode and the 2,000-μm wide electrode were connected to the driving signal and the ground, respectively. The dc voltage applied across the electrode was monitored by a digital storage oscilloscope (GW Instek, GDS-1102).

INTEGRATED UNIVERSAL ELECTRODE SYSTEM

The universal electrode system consists of a set of seven micropump structures and an electrochemical-sensing electrode located inside the mixing and sensing chamber (Figure 4). The universal electrode array was fabricated by depositing 50 nm of titanium and 150 nm of gold. The sensing electrode was then covered with scotch tape before evaporating another 50 nm of titanium and was patterned by liftoff. The height of the microchannel is 800 μm. The lengths of microchannels for pumping fluid to the central sensor chamber are between 25 and 29 mm and the width is 1 mm for all channels. The pattern was first engraved into an acrylic plate with a laser machining system (Universal Laser, Inc.). A rubber replica was then molded from the acrylic plate pattern using liquid Urethane (Forsh Polymer Corporation, 60A). The microchannel

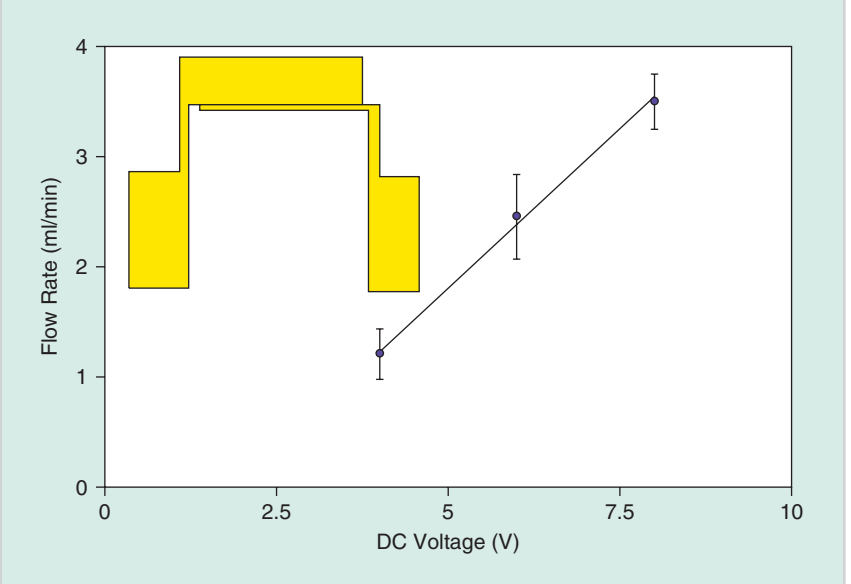

FIGURE 3 Electrolytic micropump. Influence of applied voltage on the pumping rate is illustrated. Data represent mean ± SEM. Insert shows the design of the asymmetric electrode for pumping.

The electrochemical biosensor is sensitive, specific, and rapid and represents a highly promising technology for point-of-care diagnostics of infectious diseases, such as UTIs.

was then created by polydimethylsiloxane (PDMS) molding using the replica mold. The PDMS channel and the glass substrate with the universal electrode array was bound using atmospheric plasma treatment.

RESULTS AND DISCUSSION

ELECTROLYTIC MICROPUMP

The electrolytic pumping motion is driven by the asymmetric electrode pair. When a dc current is applied to the two metal electrodes, electrolysis occurs, and the fluid is pushed by the electrolysis bubble, which transforms electrochemical energy into mechanical energy. The decomposition potential for water electrolysis is −1.23 V at 25 °C. During electrolysis, hydrogen gas is produced at the cathode, and oxygen gas is produced at the anode.

Cathode:

$$2H_2O + 2e^- \rightarrow 2OH^- + H_2(\text{gas}) \quad (1)$$

Anode:

$$2H_2O \rightarrow 4H + 4e^- + O_2(\text{gas}). \quad (2)$$

Assuming that all the generated gases grow in the form of gas bubbles, the total volume of the gas generated through bubble nucleation can be evaluated according to Faraday's law of electrolysis and the ideal gas law [17]. Theoretically, the bubble growth rate should be linearly proportional to the applied current. In our experiment, the electrolyte solution with conductivity of 1 S/m (similar to most biological buffers and physiological solutions) was used to evaluate the performance of the electrolytic micropump. The flow rate was studied and quantified as a function of the applied dc voltage (Figure 3). A flow rate on the order of milliliters per minute can be generated with only a few volts. As expected, the flow rate is found to be linearly proportional to the applied dc voltage. Extrapolation of the data reveals that the calibration curve intersects with the x-axis at ~1.8 V. The value is in reasonable agreement with the decomposition potential for water electrolysis. With the optimized channel design and electrokinetic operating conditions, the flow rate obtained in this study is at least one order of magnitude higher than that of a typical bubble-actuated micropump [18], [19].

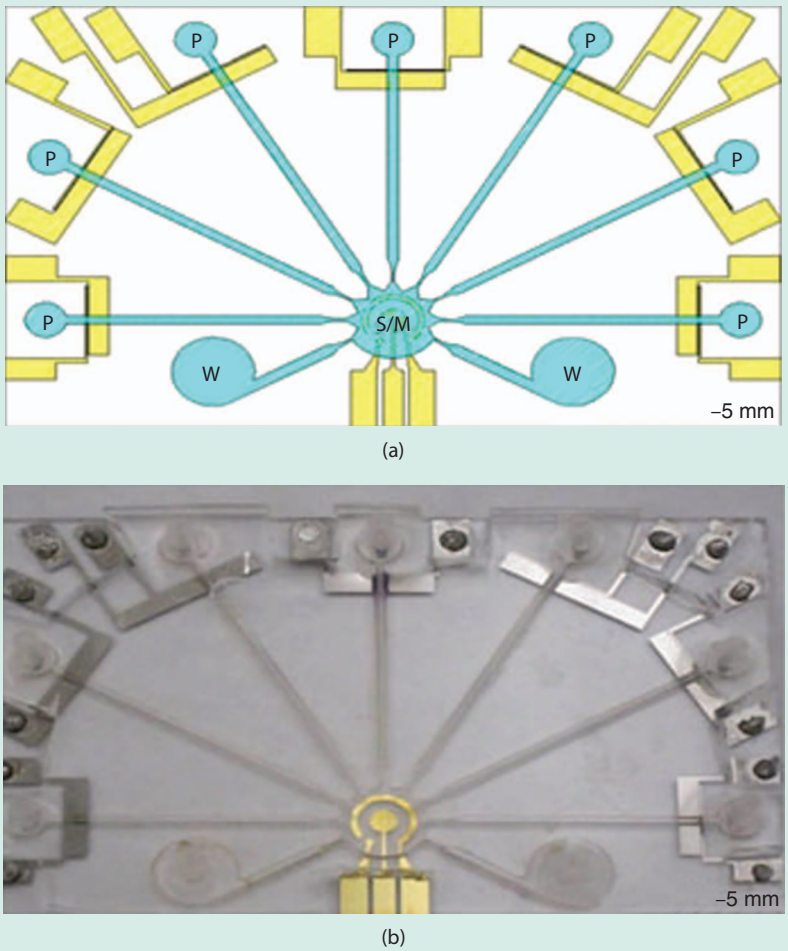

FIGURE 4 An integrated universal electrode system. (a) A schematic of the integrated microfluidic system consisting of the asymmetric pumps (P), the waste chamber (W), and the concentric electrode for both mixing and sensing modules (S/M). (b) A photograph shows the schematic design of Figure 4(a).

MICROFLUIDIC OPERATIONS WITH THE UNIVERSAL ELECTRODE

To optimize the performance of the universal electrode array for molecular analysis, color food dyes were applied to visually demonstrate the pumping, mixing, and washing efficiencies inside the integrated microfluidic systems. Color food dyes and NaCl washing solutions with conductivity of 1 S/m were loaded

in the microchannels. Figure 5(a) and (b) illustrates the motion of the food dyes toward the mixing and sensing chamber at the center of the integrated system when the electrolytic micropumps were actuated with 8-V dc. The chamber was completely filled with the color dyes. An ac square waveform at 5 Vpp and 200 kHz was then applied to the concentric electrode to enhance mixing [Figure 5(c) and (d)]. The solutions were fully mixed in less than 3 min. The mixed dye solution in the chamber was then washed by the NaCl washing solution with the corresponding electrolytic micropump with 8-V dc. The dye solution was then pushed to the waste reservoirs. The solution in the sensing and mixing chamber could be completely removed in less than 4 min. It should be noted that the universal electrode platform does not require valves to control the fluid direction.

During the washing step, the dye and NaCl solutions were preferentially driven to the waste chambers instead of other pumping channels due to the low hydrodynamic resistances of the waste chambers, which are connected to open air. The high hydrodynamic resistance in the pumping channel is a result of the closed fluid connection, which is achieved by, e.g., connecting the inlet of the micropump with a syringe or a stopper. This valveless design significantly simplifies the system complexity and completely eliminates the requirement of external pressure sources, which will facilitate the implementation of the universal electrode system for point-of-care diagnostics in the future.

INTEGRATED UNIVERSAL ELECTRODE SYSTEM

The integrated universal electrode system was applied to implement the electrochemical assay for detecting bacterial 16S rRNA. *Escherichia coli* (*E. coli*) clinical isolates from UTI patients were chosen as the model system. All solutions were delivered using the electrolytic pump. The reagents include the bacterial lysate solution (*E. coli* mixed with the lysis buffer and 1 M NaOH), the detector probe solution, the enzyme solution, and the NaCl solution with conductivity of 1 S/m (Figure 6). The mixing and sensing chamber in the integrated system was washed once with the NaCl washing solution after each incubation step. The hybridization and immobilization steps were performed on the electrochemical sensor with and without electrokinetic mixing and assay enhancement. The results were compared with the assay performed manually with pipettes as in our previous studies

> The flow rate obtained in this study is at least one order of magnitude higher than that of a typical bubble-actuated micropump.

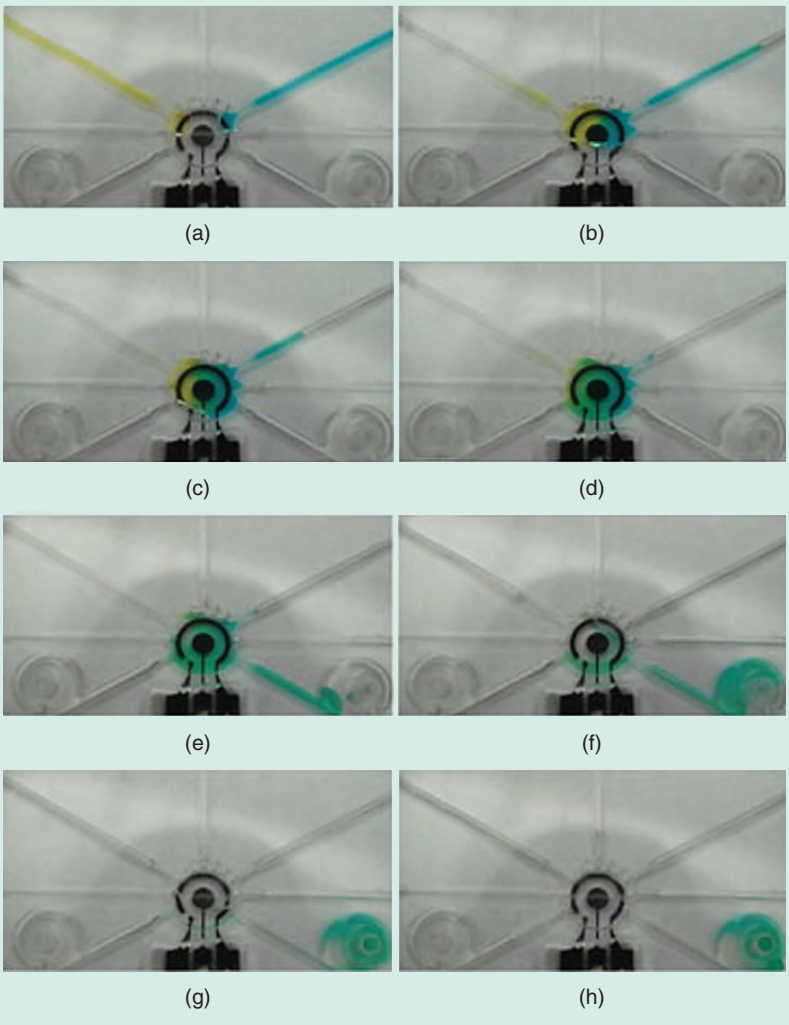

FIGURE 5 Microfluidic operations in the universal electrode platform. (a) and (b) Electrolytic pumping of two color food dyes into the mixing and sensing chamber. (c) and (d) Electrokinetic mixing of the color food dyes is performed directly on top of the electrochemical-sensing electrode. (e)–(h) A washing buffer is loaded into the channel using the electrolytic pump and delivered to the waste reservoirs.

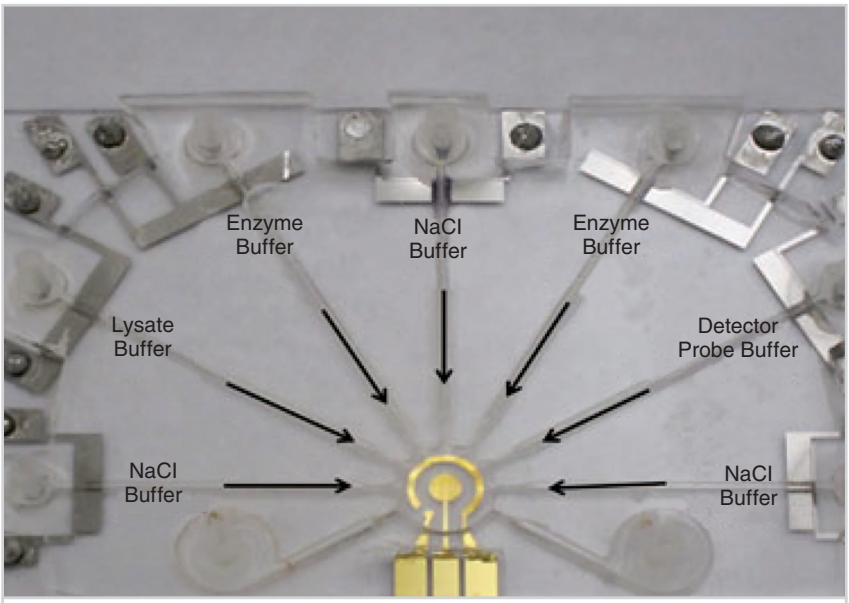

FIGURE 6 The configuration of the universal electrode array for implementing the electrochemical assay for bacterial 16S rRNA.

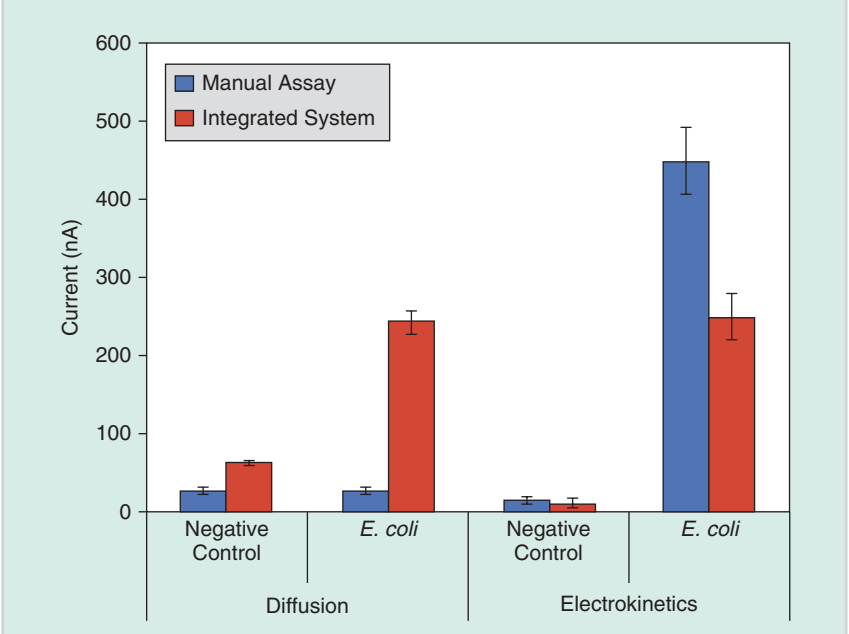

FIGURE 7 A comparison of the electrochemical assays performed manually or by the integrated universal electrode system.

[12]–[14]. For the manual assay, the sensing chamber was an acrylic well and was washed three times after each incubation step. The target concentration was equivalent to 4×10^5 colony-forming units per sensor in both the manual assay and the integrated system.

The performance of electrokinetic mixing for enhancing the 16S rRNA hybridization assay was evaluated. The signals of the 16S rRNA assays performed with electrokinetic enhancement and by diffusion are shown in Figure 7. In the manual assay, the signal level without electrokinetic enhancement was similar to the negative control due to the lack of an efficient mixing mechanism. In the integrated system, electrokinetic enhancement significantly reduced the background noise in the negative control and improved the overall signal-to-noise ratio. The noise reduction was a result of the elevated temperature and electrothermal stringency wash [9]. These results indicate that in situ electrokinetic enhancement can improve the signal-to-noise ratio of the electrochemical assay inside the integrated universal electrode system. The ability to perform in situ electrokinetic enhancement can simplify the assay protocol and facilitate molecular analysis at the point of care.

The signals obtained from the integrated system were compared with the manual assay. With diffusion, the signal and noise levels were both increased in the integrated system compared with the manual assay. The higher signal level could be due to the shorter diffusion distance in the integrated system, and the higher noise level could be due to the smaller number of washes and the lower washing efficiency in the integrated system. In contrast, with electrokinetics, both the signal and noise levels were reduced in the integrated microfluidic system. It should be noted that the height of the integrated chip is 800 μm, which is 2.5 times lower than that of the acrylic well in the manual assay (2 mm). The lower current level is likely due to the differences in channel geometries, which could affect the quasi-steady-state substrate concentration.

The smaller dimension may also play a role in the mixing effect, which is driven by the bulk fluid motion. Furthermore, the higher surface-to-volume ratio in the integrated system implies a larger temperature loss, which may modify the optimal condition for generating the electrothermal fluid motion for mixing and assay enhancement. Nevertheless, the signal-to-noise level is comparable between the integrated system and the manual assay in the experiment. These results demonstrate the applicability of the universal electrode system in molecular diagnostics.

The valveless design dramatically simplifies the system's complexity and cost, both of which are essential for point-of-care diagnostics.

DISCUSSION

In this study, we demonstrated a universal electrode approach for microfluidics-based molecular biosensing. Using the universal electrode platform, all fundamental microfluidic operations, such as pumping, mixing, washing, enhancement, and sensing, can be performed for molecular diagnostics. The asymmetric micropump design is capable of generating a large volumetric flow rate that is an order of magnitude higher than that generated by conventional electrolytic micropumps. Furthermore, the valveless design dramatically simplifies the system's complexity and cost, both of which are essential for point-of-care diagnostics. The ability to directly perform in situ mixing and enhancement on the sensor electrode further simplifies the system complexity. Since only electronic interfaces are required to implement the universal electrode approach, the bulky supporting equipment required in typical bioanalytical settings is eliminated, facilitating the implementation of microfluidics-based bioanalysis in resource-limited settings.

CONCLUSION

In this article, we demonstrated a universal electrode approach for automating bioanalytical assays toward point-of-care diagnostics. Our work presents a novel approach for implementing both sample preparation and electrochemical sensing steps on the same universal electrode platform. With its general applicability and effectiveness, the universal electrode approach is anticipated to implement various microfluidics-based bioanalytical assays for point-of-care diagnostics.

ACKNOWLEDGMENT

This work is supported by the National Institutes of Health (NIH) (1U01AI082457-01; 2R44AI088756-03), the NIH Director's New Innovator Award (1DP2OD007161-01), and the National Science Foundation (0930900).

ABOUT THE AUTHORS

Mandy L. Y. Sin (mandysin@stanford.edu.) is with the Department of Aerospace and Mechanical Engineering, University of Arizona, Tucson, and with the Department of Urology, Stanford University, Palo Alto, California.

Vincent Gau (vgau@genefluidics.com) is with GeneFluidics, Inc., Irwindale, California.

Joseph C. Liao (jliao@stanford.edu) is with the Department of Urology, Stanford University, Palo Alto, California.

P. K. Wong (pak@email.arizona.edu) is with the Department of Aerospace and Mechanical Engineering, University of Arizona, Tucson.

REFERENCES

[1] M. L. Sin, J. Gao, J. C. Liao, and P. K. Wong, "System integration: A major step toward lab on a chip," *J. Biol. Eng.*, vol. 5, p. 6, 2011.

[2] R. Mariella, "Sample preparation: The weak link in microfluidics-based biodetection," *Biomed. Microdevices*, vol. 10, pp. 777–784, Dec. 2008.

[3] G. Whitesides, "Solving problems," *Lab Chip*, vol. 10, pp. 2317–2318, 2010.

[4] T. H. Wang and P. K. Wong, "Transforming microfluidics into laboratory automation," *J. Assoc. Lab. Autom.*, vol. 15, pp. A15–A16, 2010.

[5] P. K. Wong, T. H. Wang, J. H. Deval, and C. M. Ho, "Electrokinetics in micro devices for biotechnology applications," *IEEE/ASME Trans. Mechatron.*, vol. 9, pp. 366–376, June 2004.

[6] A. Ramos, H. Morgan, N. G. Green, and A. Castellanos, "AC electrokinetics: A review of forces in microelectrode structures," *J. Phys. D, Appl. Phys.*, vol. 31, pp. 2338–2353, Sept. 1998.

[7] J. Gao, M. L. Y. Sin, T. Liu, V. Gau, J. C. Liao, and P. K. Wong, "Hybrid electrokinetic manipulation in high-conductivity media," *Lab Chip*, vol. 11, no. 10, pp. 1770–1775, 2011.

[8] S. Park, Y. Zhang, T. H. Wang, and S. Yang, "Continuous dielectrophoretic bacterial separation and concentration from physiological media of high conductivity," *Lab Chip*, vol. 11, pp. 2893–2900, 2011.

[9] M. L. Sin, T. Liu, J. D. Pyne, V. Gau, J. C. Liao, and P. K. Wong, "In situ electrokinetic enhancement for self-assembled-monolayer-based electrochemical biosensing," *Anal. Chem.*, vol. 84, pp. 2702–2707, Mar. 2012.

[10] M. L. Y. Sin, V. Gau, J. C. Liao, and P. K. Wong, "Electrothermal fluid manipulation of high-conductivity samples for laboratory automation applications," *J. Assoc. Lab. Autom.*, vol. 15, pp. 426–432, 2010.

[11] A. Sonnenberg, J. Y. Marciniak, R. Krishnan, and M. J. Heller, "Dielectrophoretic isolation of DNA and nanoparticles from blood," *Electrophoresis*, vol. 33, pp. 2482–2490, Aug. 2012.

[12] R. Mohan, K. E. Mach, M. Bercovici, Y. Pan, L. Dhulipala, P. K. Wong, and J. C. Liao, "Clinical validation of integrated nucleic acid and protein detection on an electrochemical biosensor array for urinary tract infection diagnosis," *PLoS One*, vol. 6, p. e26846, 2011.

[13] K. E. Mach, R. Mohan, E. J. Baron, M. C. Shih, V. Gau, P. K. Wong, and J. C. Liao, "A biosensor platform for rapid antimicrobial susceptibility testing directly from clinical samples," *J. Urol.*, vol. 185, pp. 148–153, Jan. 2011.

[14] Y. Pan, G. A. Sonn, M. L. Sin, K. E. Mach, M. C. Shih, V. Gau, P. K. Wong, and J. C. Liao, "Electrochemical immunosensor detection of urinary lactoferrin in clinical samples for urinary tract infection diagnosis," *Biosens. Bioelectron.*, vol. 26, pp. 649–654, Oct. 2010.

[15] K. E. Mach, P. K. Wong, and J. C. Liao, "Biosensor diagnosis of urinary tract infections: A path to better treatment?," *Trends Pharmacol. Sci.*, Mar. 2011.

[16] K. E. Mach, C. B. Du, H. Phull, D. A. Haake, M. C. Shih, E. J. Baron, and J. C. Liao, "Multiplex pathogen identification for polymicrobial urinary tract infections using biosensor technology: A prospective clinical study," *J. Urol.*, Oct. 2009.

[17] C. T. Ho, R. Z. Lin, H. Y. Chang, and C. H. Liu, "Micromachined electrochemical T-switches for cell sorting applications," *Lab Chip*, vol. 5, pp. 1248–1258, 2005.

[18] C. M. Cheng and C. H. Liu, "An electrolysis-bubble-actuated micropump based on the roughness gradient design of hydrophobic surface," *J. Microelectromech. Syst.*, vol. 16, pp. 1095–1105, Oct. 2007.

[19] C. H. Liu, S. C. Chan, and C. R. Chen, "A bubble-activated micropump with high-frequency flow reversal," *Sens. Actuators A, Phys.*, vol. 163, pp. 501–509, Oct. 2010.